IEEE Access
Multidisciplinary | Rapid Review | Open Access Journal

SPECIAL SECTION ON CHALLENGES AND ENDEAVORS OF RADIATED RADIO FREQUENCY TESTS FOR 5G RADIOS

Received June 23, 2020, accepted July 19, 2020, date of publication August 10, 2020, date of current version August 21, 2020.

Digital Object Identifier 10.1109/ACCESS.2020.3015231

Implications of Incident Power Density Limits on Power and EIRP Levels of 5G Millimeter-Wave User Equipment

WANG HE[1], BO XU[2,3], (Member, IEEE), YUANQING YAO[1], DAVIDE COLOMBI[2], ZHINONG YING[4], (Senior Member, IEEE), AND SAILING HE[1,3], (Fellow, IEEE)

[1]Centre for Optical and Electromagnetic Research, Zhejiang University, Hangzhou 310058, China
[2]Ericsson Research, Ericsson AB, 164 80 Stockholm, Sweden
[3]Department of Electromagnetic Engineering, KTH Royal Institute of Technology, 100 44 Stockholm, Sweden
[4]Sony Research Center, Sony Corporation, 221 88 Lund, Sweden

Corresponding author: Sailing He (sailing@kth.se)

This work was supported in part by the National Key Research and Development Program of China under Grant 2018YFC1407503, in part by the National Natural Science Foundation of China under Grant 11621101, and in part by the Fundamental Research Funds for the Central Universities (Zhejiang University NGICS Platform).

ABSTRACT User equipment (UE) is required to comply with the relevant radio frequency (RF) electromagnetic field (EMF) exposure limits, which are of relevance to establish the maximum permissible transmitted power and the maximum equivalent isotropically radiated power (EIRP). Recently, international RF EMF exposure guidelines, such as those published by the International Commission on Non-Ionizing Radiation Protection (ICNIRP) as well as by the IEEE, have been updated. In this paper, the implications of the revised incident power density limits are investigated in terms of maximum permissible transmitted power and the maximum EIRP for devices operating in close proximity of the user. A similar analysis is conducted according to the US Federal Communications Commission (FCC) regulation on RF exposure. EMF compliance of UE is studied by means of numerical modelling of patch antenna arrays of different array sizes taking into consideration of possible beam-steering operations, at frequencies ranging from 10 GHz to 100 GHz. The results are compared with the 3rd Generation Partnership Project (3GPP) requirements on the total radiated power (TRP) and EIRP levels. The present implications of the incident power density limits for 5G millimeter-wave UE will give valuable insights to mobile equipment manufacturers, network operators, and standardization bodies.

INDEX TERMS 5G, antenna array, beam-steering, EIRP, incident power density, maximum permissible transmitted power, millimeter wave, RF EMF exposure, user equipment.

I. INTRODUCTION

The fifth-generation (5G) mobile communication technology, i.e., New Radio (NR), utilizes millimeter-wave (mmWave) frequencies as well as part of the frequency spectrum below 6 GHz [1], [2]. Since mmWave is characterized by larger free-space path loss than the sub-6 GHz bands [3], antenna arrays are employed to achieve higher antenna gain and narrow directional beams. To ensure spatial coverage, beam-steering techniques are used by controlling the phase of each antenna element in the user equipment (UE) [4]–[11].

The radio frequency (RF) electromagnetic field (EMF) exposure from UE is required to comply with the relevant RF EMF exposure limits. In October 2019, the IEEE published IEEE Std C95.1^{TM} [12] based on the revisions of [13] (2005) and [14] (2002). In April 2020, the International Commission on Non-Ionizing Radiation Protection (ICNIRP) published the revised guidelines to limit EMF exposure in the frequency range 100 kHz to 300 GHz [15]. This document updates the RF EMF part of the ICNIRP guidelines of 1998 [16], and the 100 kHz to 10 MHz part of the ICNIRP low frequency guidelines [17] from 2010. Although the limits specified in the new guidelines are, to a large extent, the same as those previously available, both the IEEE and the ICNIRP include some changes in the RF EMF exposure limits above 6 GHz,

The associate editor coordinating the review of this manuscript and approving it for publication was Xiaoming Chen.

for which the implications on 5G UE compliance are investigated in this work. In the US, the RF exposure limits set by the Federal Communications Commission (FCC) apply and are also addressed in the paper.

In addition to practical factors that limit the maximum output power of UE, such as power amplifiers and battery life, the maximum permissible transmitted power, P_{MPT}, and the maximum equivalent isotropically radiated power, $EIRP_{\mathrm{max}}$, should ensure that RF EMF exposure of UE is in compliance with the relevant exposure limits. At the same time, the total radiated power (TRP) and EIRP of the UE should also meet the 3rd Generation Partnership Project (3GPP) requirements to support sufficient coverage and limit interference [18].

Previous studies investigated the implications of the exposure limits on P_{MPT} and $EIRP_{\mathrm{max}}$ levels. In [19], dipole arrays of different sizes ranging from 2×2 to 10×10 elements in the frequency range 10 GHz to 60 GHz, were analyzed. In [20], RF EMF exposure and P_{MPT} were addressed for UE antenna arrays of 15 GHz and 28 GHz. Recently, the impacts of the UE antenna casing on EMF compliance were studied [21] for 28 GHz and 39 GHz UE. However, since existing studies were conducted before IEEE and ICNIRP published their revised limits, some of the conclusions previously drawn need to be reassessed.

In this paper, we use patch arrays with different sizes and operating frequencies ranging from 10 GHz to 100 GHz to estimate P_{MPT} and $EIRP_{\mathrm{max}}$ levels of UE in order to comply with the latest EMF exposure standards and regulations. These values are then compared with relevant requirements from 3GPP applicable for 5G mmWave UE. The provided P_{MPT} and $EIRP_{\mathrm{max}}$ levels can be used when manufactures and operators plan for 5G mmWave products and standardization bodies make specifications on UE power levels.

II. MODEL AND METHOD

A. RF EMF EXPOSURE LIMITS ABOVE 6 GHz

RF EMF exposure limits from 10 MHz to 300 GHz are set to protect people from established adverse health effects associated with body core temperature rise and excessive localized heating. RF EMF exposure metrics limiting local exposure are considered of relevance to UE. Above 6 GHz, ICNIRP *basic restrictions* [15] and IEEE *dosimetric reference limits* (DRLs) [12] for local exposure are defined in terms of absorbed and epithelial power density, respectively. The absorbed power density is defined as the spatial-average Poynting vector projected in the direction normal to the averaging area on the body surface. The epithelial power density is defined as the power flow through the epithelium per unit area directly under the body surface. Although expressed with different terms, absorbed and epithelial power density represent the same quantity. As basic restrictions/DRLs cannot be easily assessed, IEEE and ICNIRP provide additional limits, i.e., *reference levels* or *exposure reference limits* (ERLs) using quantities that are more practical to evaluate. Above 6 GHz, reference levels/ERLs, as well as the RF exposure limits specified by the FCC, are defined in terms of incident power density. Compliance assessment of UE based on such metric has been extensively studied, e.g., [22]–[29].

In the ICNIRP 2020 guidelines, the incident power density limits for general public are $55f_{\mathrm{G}}^{-0.177}\mathrm{W/m^2}$ in the frequency range 6–300 GHz (f_{G} is the frequency in the unit of GHz). The incident power density averaged over 4 $\mathrm{cm^2}$ of the body surface in the shape of a square should not exceed the limit values. In addition, above 30 GHz, the incident power density averaged over a square 1 $\mathrm{cm^2}$ should not exceed twice that of the 4 $\mathrm{cm^2}$ restrictions, i.e., $110f_{\mathrm{G}}^{-0.177}\mathrm{W/m^2}$.

IEEE Std C95.1™-2019 also has the same 4 $\mathrm{cm^2}$ spatial-averaging restrictions as the ICNIRP 2020 guidelines. Above 30 GHz, if the area of the -3 dB contour relative to the peak spatial incident power density is less than 1 $\mathrm{cm^2}$, the incident power density averaged over 1 $\mathrm{cm^2}$ should not exceed twice the 4 $\mathrm{cm^2}$ limits, either.

The Maximum Permissible Exposure (MPE) limits for incident power density set by the FCC is 10 $\mathrm{W/m^2}$ for the general population [30]. According to the current FCC compliance assessment procedures applicable for mmWave handsets, this is intended to be averaged over 4 $\mathrm{cm^2}$ [31], [32]. In the following, we refer to such requirements as 'FCC (current)'. While this limit value is derived from the MPE applicable for whole-body exposure, FCC rules do not yet specify a spatial maximum power density limit for local exposure above 6 GHz. Therefore, for local exposure, the FCC has recently proposed a general local power density limit of 40 $\mathrm{W/m^2}$ averaged over 1 $\mathrm{cm^2}$ above 6 GHz [33]. In the following, we refer to them as 'FCC (proposed)'. Table 1 summaries the recently updated ICNIRP and IEEE incident power density limits, and the restrictions currently in use and recently proposed by the FCC.

TABLE 1. Localized Inicident Power Density Limits set by ICNIRP, IEEE, and FCC for General Public above 6 GHz.

	f_{G} (GHz)	Averaging area ($\mathrm{cm^2}$)	S_{lim} ($\mathrm{W/m^2}$)
ICNIRP 2020 [15]	6–300	4	$55f_{\mathrm{G}}^{-0.177}$
	30–300	1	$110f_{\mathrm{G}}^{-0.177}$
IEEE C95.1™-2019 [12]	6–300	4	$55f_{\mathrm{G}}^{-0.177}$
	30–300 [a]	1	$110f_{\mathrm{G}}^{-0.177}$
FCC (current) [30]–[32]	6–100	4	10
FCC (proposed) [33]	6–3000	1	40

[a] According to IEEE C95.1™-2019, 1 $\mathrm{cm^2}$ averaging is required only when the area of the -3 dB contours relative to the peak spatial incident power density is less than 1 $\mathrm{cm^2}$.

Fig. 1 shows an example of the incident power density calculation over an averaging area A at a distance d, where the surface of interest is chosen parallel to the array in this paper. For a progressive phase shift difference of β_x between adjacent elements in the x-direction, the spatial-average incident power density, according to IEEE Std C95.1™-2019 and

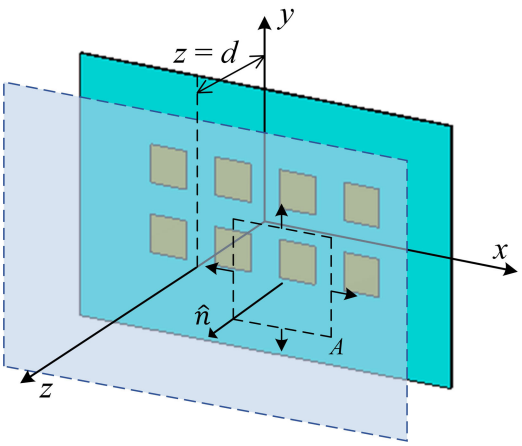

FIGURE 1. Illustration for the calculation of spatial-average incident power density.

the ICNIRP 2020 guidelines,[1] can be expressed as:

$$S_{\text{inc}}(A, d, \beta_x) = \frac{1}{A}\int_A \text{Re}\left[\boldsymbol{E}(d, \beta_x) \times \boldsymbol{H}^*(d, \beta_x)\right] \cdot \hat{\boldsymbol{n}}\, \text{d}s, \quad (1)$$

where $\boldsymbol{E}$ and $\boldsymbol{H}$ are the root-mean-square (rms) complex electric field and the rms complex magnetic field, respectively, superscript * denotes the complex conjugation, and $\hat{\boldsymbol{n}}$ is the unit vector normal to the averaging area.

The FCC currently requires three orthogonal components of the Poynting vector to determine compliance [34] against the incident power density limits, which can be expressed as:

$$S_{\text{inc}}^{\text{m}}(A, d, \beta_x) = \frac{1}{A}\int_A \left|\text{Re}\left[\boldsymbol{E}(d, \beta_x) \times \boldsymbol{H}^*(d, \beta_x)\right]\right| \text{d}s. \quad (2)$$

For brief exposure intervals, the ICNIRP and IEEE Std C95.1™-2019 specify reference levels (or ERLs) also in terms of incident energy density. As in this paper, exposure assessment is conducted assuming the UE constantly transmitting at the maximum output power, compliance with the incident energy density limits is inherently met by complying with the incident power density limits.

B. ARRAY CONFIGURATION AND TOPOLOGY

Patch antenna arrays and other patch-antenna-based designs are popular choices for 5G UE above 6 GHz (e.g., [9]–[11]), as they are compatible with the printed circuit board (PCB) and packaging technologies. As the number of antenna elements is usually with the power of two in practice, we select the array sizes of 2 × 2, 4 × 1, 4 × 2, 4 × 4, 8 × 1, 8 × 2, 8 × 4, 8 × 8, 16 × 8, and 16 × 16 in this paper. Fig. 2 shows the dimensions of the 4 × 2 patch antenna array as an example. The dimensions of antenna elements and the distances of element spacing are the same in wavelength for different frequencies and array sizes. The patch elements are square-shaped with a side length of $0.31\lambda_0$, and the element spacing is $0.57\lambda_0$ (this allows for a ±60° array scanning range), where λ_0 is the free space wavelength at the operating frequency. The permittivity and the thickness of the substrate are 2.2 and $\lambda_0/50$, respectively. Each patch antenna is excited by a coaxial probe feed, of which the position is indicated by the red spot in Fig. 2. The operating frequencies are chosen from 10 GHz to 100 GHz for every 5 GHz.

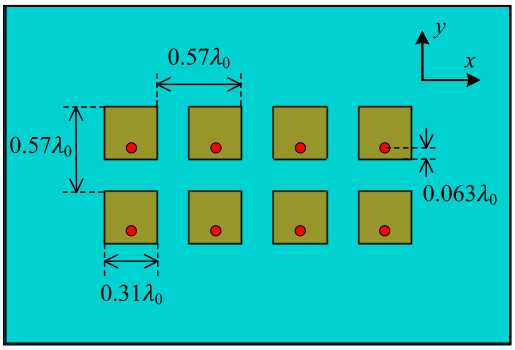

FIGURE 2. An array configuration example: 4×2 patch array.

Beam steering is considered in the xz-plane. The progressive phase shift between the horizontal adjacent elements is $\beta_x \in [0, \pi]$ with the step size of $\pi/2N_x$ to achieve the scanning range in [0°, 60°], where N_x is the element number along the x-direction.

C. MAXIMUM PERMISSIBLE TRANSMITTED POWER DUE TO INCIDENT POWER DENSITY LIMITS

For large array antennas, the maximum exposure may occur at some distance away from the face of the antenna, as suggested in Appendix A. When the P_{MPT} and $EIRP_{\text{max}}$ results are presented for a certain distance d, it is understood that compliance is ensured for all distances larger or equal to this distance. Therefore, the compliance with the incident power density limits is assessed considering the distances ranging from 5 mm to 50 cm for 2 × 2, 4 × 1, 4 × 2, 4 × 4, 8 × 1, 8 × 2, 8 × 4, and 8 × 8 arrays and from 5 mm to 90 cm for 16 × 8 and 16 × 16 arrays. The areas for spatial averaging are chosen parallel to the face of the antenna array, and the distance between them is the evaluation distance d (see Fig. 1). The P_{MPT} level for d is determined by the maximum peak spatial-average incident power density for $d' \geq d$ and all β_x. For the incident power density limits, S_{lim}, in Table 1, P_{MPT} could be expressed as

$$P_{\text{MPT}} = \frac{P_{\text{f}} S_{\text{lim}}}{\max\limits_{A, d' \geq d, \beta_x} S_{\text{inc}}(A, d', \beta_x)}, \quad (3)$$

where P_{f} is the total forward power in simulation, i.e., the generated power of the RF front end. S_{inc} in (3) may be replaced with that in (2) when determining P_{MPT} for the FCC requirements. Note that P_{MPT} in (3) is not considered for the restrictions of EIRP and TRP discussed below, and it is the

[1] In the ICNIRP 2020 guidelines, incident power density is defined as the modulus of the complex Poynting vector. However, it also states that: "In near-field exposure scenarios, the components of the Poynting vector are not real values but complex ones. In such cases a detailed investigation of the Poynting vector components may be necessary to calculate the incident power density relevant to radiofrequency safety." Therefore, in this paper, we apply the IEEE definition for the incident power density when determining compliance for the ICNIRP limits for portable and mobile device applications.

TABLE 2. 3GPP Requirements of Minimum Peak EIRP, Maximum EIRP, and Maximum TRP for Different UE Power Classes (3GPP TS 38.101-2 v15.9.1 [18].

3GPP UE Power Class	Frequency	Minimum Peak EIRP	Maximum TRP	Maximum EIRP
Power Class 1 (Fixed wireless access UE)	24.25–29.5 GHz (n257, n258, n261)	40 dBm	35 dBm	55 dBm
	37–40 GHz (n260)	38 dBm		
Power Class 2 (Vehicular UE)	24.25–29.5 GHz (n257, n258, n261)	29 dBm	23 dBm	43 dBm
Power Class 3 (Handheld UE)	24.25–29.5 GHz (n257, n258, n261)	22.4 dBm	23 dBm	43 dBm
	37–40 GHz (n260)	20.6 dBm		
Power Class 4 (High power non-handheld UE)	24.25–29.5 GHz (n257, n258, n261)	34 dBm	23 dBm	43 dBm
	37–40 GHz (n260)	31 dBm		

sum of accepted power and reflected power of the antenna array. The total efficiency for the arrays as β_x varies can be found in Appendix B, which can be used to scale P_{MPT} to the total accepted power.

The results are presented particularly for d of 5 mm and 20 cm from the antenna surface. For UE intended to be operating in close proximity to individuals, the FCC has different RF exposure evaluation requirements on two classes of equipment, namely the portable devices [35] and mobile devices [36]. A portable device, such as a mobile handset, is defined as a transmitting device designed to be used so that the radiating structure(s) of the device is/are within 20 cm of the body of the user [35]. A mobile device, such as customer-premises equipment (CPE), is defined as a transmitting device designed for use in other than fixed locations and generally in such a way that a separation distance of at least 20 cm is normally maintained between the antennas and exposed individuals [36]. The UE categorized as a mobile device can still have a larger compliance distance than 20 cm, and the $EIRP_{\text{max}}$ levels can be higher than what is suggested in Appendix D but may still need to comply with the relevant FCC limits in the US.

D. EIRP RESTRICTIONS

Using (3), the maximum EIRP for the beam-steering antenna array is calculated with

$$EIRP_{\text{max}} = P_{\text{MPT}} \times \max_{\beta_x} \left(G(\beta_x)\right), \tag{4}$$

where G is the realized antenna array gain, as P_{MPT} is derived from the forward power.

In the current deployed 5G NR frequency range 2 (FR2) (including bands n257, n258, n260, and n261), 3GPP specifies the minimum peak EIRP, maximum EIRP, and maximum TRP levels on different UE power classes, see Table 2 [18]. 5G UE should fulfil both the 3GPP requirements and the EMF exposure restrictions in terms of P_{MPT}. The UE power class 3 is for handheld UE, for which $d = 5$ mm is assumed in this paper. The UE power classes 2 and 4 are for vehicular UE and high-power non-handheld UE, respectively. $d = 20$ cm is considered for them to be aligned with minimum requirement of the FCC mobile devices. In this paper, it is assumed that the limits identified as 'FCC (proposed)' will apply, if adopted, to UE relevant for power class 3 as well as classes 2 and 4. Power class 1 is for fixed wireless access UE, which does not typically operate in close proximity of the body and are therefore outside the scope of this paper.

E. SIMULATION SCHEME

The full-wave simulations are conducted using CST Suite Studio [38] with the time domain solver (T-solver) based on the finite integration technique (FIT), the asymptotic solver (A-solver) based on the shooting and bouncing rays (SBR), and the integral equation solver (I-solver) based on the method of moments (MoM). The fields and incident power density of interest are up to a distance of 90 cm, and such distance is $30\lambda_0$ at 10 GHz and $300\lambda_0$ at 100 GHz. If only using the T-solver to compute the fields, the requirements on hardware will be very demanding, and the simulation tasks will be extremely time-consuming. For P_{MPT} and $EIRP_{\text{max}}$ calculations, only the information regarding the maximum peak spatial-average incident power density, rather than the entire field distribution, is needed. To capture the peak spatial-average incident power density, a simulation scheme is developed to accelerate the simulation process, see the flow chart in Fig. 3. The control flow and post-processing of the field results are performed in MATLAB [39].

For each frequency, each array size, and each beam, the T-solver is used to compute the far-field beam patterns and the equivalent field sources over a closed box with a $\lambda_0/4$ distance surrounding the array. The equivalent field sources are then imported into the A-solver, and the incident power density is computed on a series of planes normal to the z-axis in the distance range of $d \in (\lambda_0, 50\text{ cm}]$ for 2×2, 4×1, 4×2, 4×4, 8×1, 8×2, 8×4, and 8×8 arrays and $d \in (\lambda_0, 90\text{ cm}]$ for 16×8 and 16×16 arrays. Due to the relatively large uncertainty of the A-solver, the incident power density computed in the A-solver is only used to locate the approximate position of the peak spatial-average incident power density. More accurate results around the approximate position are computed using the I-solver with the equivalent field sources in a limited volume to reduce simulation time. In the distance range of $d \in (\lambda_0/4, \lambda_0]$, the A-solver is not used due to the relatively poor accuracy, and the fields are computed in the I-solver using the equivalent field sources around the array

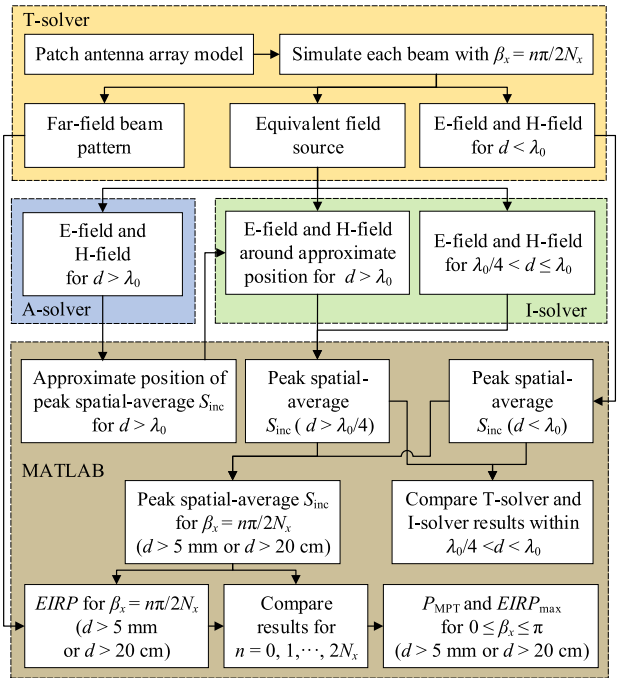

FIGURE 3. Flow chart for the computation of P_{MPT} and $EIRP_{max}$.

aperture. The field sampling interval is no larger than the minimum between 1 mm and $\lambda_0/8$ for $d \in [5\text{ mm}, \lambda_0]$, and no larger than the minimum between 2 mm and $\lambda_0/2$ for $d > \lambda_0$. At those frequencies with $\lambda_0/4 \ge 5$ mm, the field data in the range of $d \in [5\text{ mm}, \lambda_0/4]$ is supplemented by the T-solver results. The comparison of the peak spatial-average incident power density directly computed in the T-solver and that computed in the I-solver with the equivalent field sources can be found in Appendix C.

III. RESULTS

A. AVERAGING AREA SIZE DETERMINING COMPLIANCE FOR ICNIRP AND IEEE LIMITS

Both the ICNIRP and the IEEE specify power density limits above 30 GHz intended to be averaged over 1 cm^2 and 4 cm^2. The limit value applicable to 1 cm^2 is twice of that provided for 4 cm^2 and is therefore relevant only for small exposure areas. The IEEE provides a criterion to identify very localized exposure, for which an averaging area of 1 cm^2 is relevant (in addition to 4 cm^2) based on the -3 dB contour area of the incident power density. An example is given in Fig. 4.

For the investigated antenna arrays, the averaging area that determines P_{MPT} and the resultant $EIRP_{max}$ levels are found no difference between the ICNIRP and IEEE requirements. Fig. 5 shows the averaging area size that determines P_{MPT} for $d = 5$ mm. In general, above 30 GHz, the 1 cm^2 requirement determines P_{MPT} for small size arrays. As the array size increases and the transmitted power is spread over a larger area, the 4 cm^2 requirement determines P_{MPT} in the relatively low frequency range. For $d = 20$ cm, the 4 cm^2 requirement determines P_{MPT} for both the ICNIRP and IEEE requirements and for all arrays and frequencies investigated

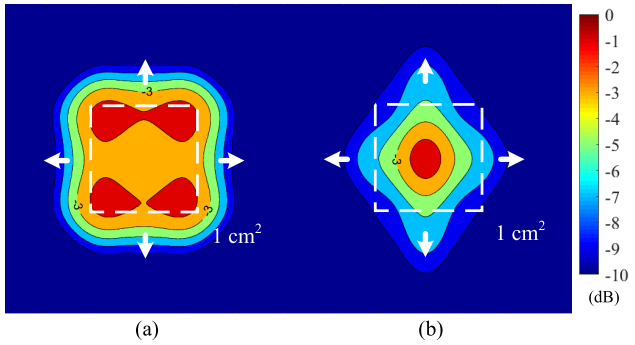

FIGURE 4. Example of determination of the averaging area for the 4 × 4 patch antenna array at 40 GHz. (a) The −3 dB contour area is larger than 1 cm^2 (according to the IEEE only the limit on 4 cm^2 applies); (b) The −3 dB contour area is smaller than 1 cm^2 (according to the IEEE both the limits on 4 cm^2 and 1 cm^2 are applicable).

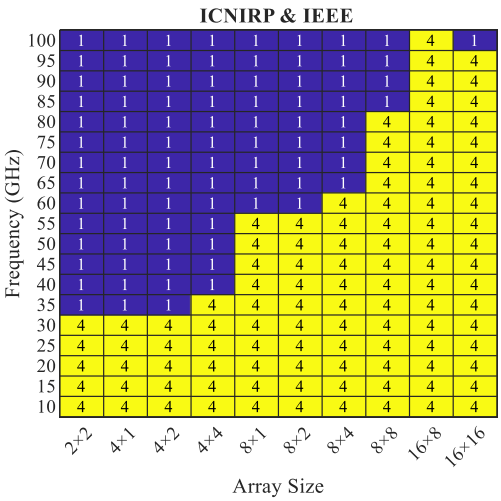

FIGURE 5. Averaging area for determining P_{MPT} to comply with the ICNIRP and IEEE requirements for $d = 5$ mm.

in this paper, as the field distribution is nearly uniform within an averaging area.

B. MAXIMUM PERMISSIBLE TRANSMITTED POWER

Fig. 6 shows P_{MPT} for $d = 5$ mm to be compliant with the ICNIRP, IEEE, current FCC, and proposed FCC limits. As found in the previous work [19], for the same array topology, P_{MPT} declines with the increasing frequency. This is because the power is more focused at short distances as the physical size of the array is reduced. At the same frequency, P_{MPT} is higher for a larger array size, as the power is more spread in space. The same trend can also be found in this paper as shown in Fig. 6. However, comparing the results between the 4 × 1 and 4 × 2 array, and between the 8 × 1 and 8 × 2 array, the P_{MPT} levels for the 4 × 1 and 8 × 1 arrays are higher than those for the 4 × 2 and the 8 × 2 arrays, respectively. This is because the one-dimensional linear array only has constructive field superposition in one direction, while the two-dimensional array with constructive field superposition in two orthogonal directions results in more enhanced field strength at close distances.

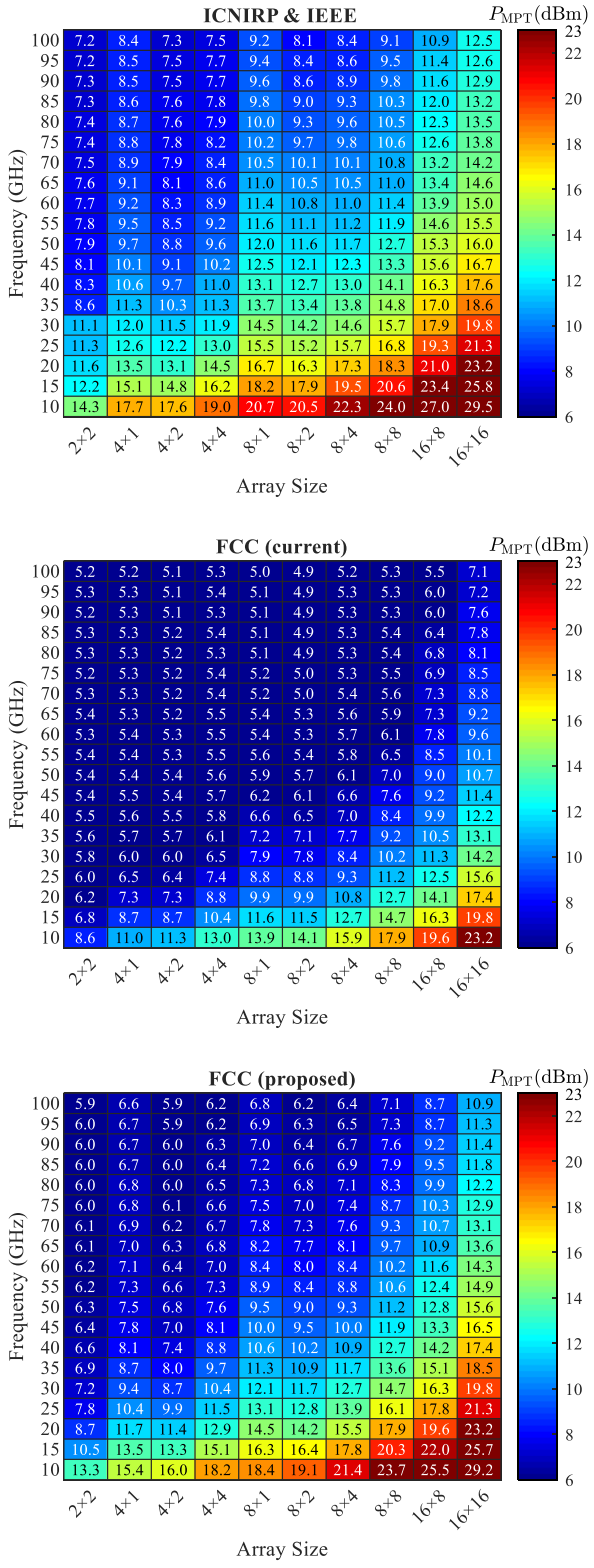

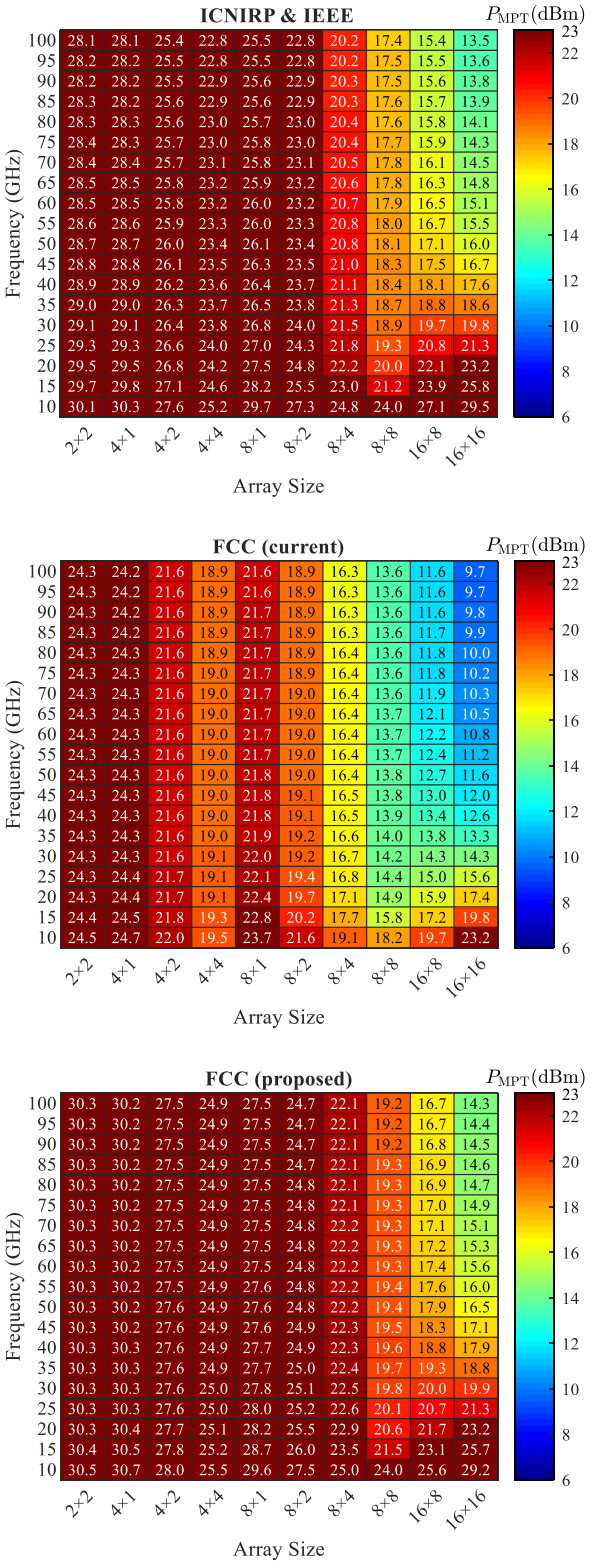

FIGURE 6. P_{MPT} levels for $d = 5$ mm to comply with the incident power density limits of ICNIRP, IEEE, FCC (current), and FCC (proposed).

FIGURE 7. P_{MPT} levels for $d = 20$ cm to comply with the incident power density limits of ICNIRP, IEEE, FCC (current), and FCC (proposed).

The P_{MPT} levels for $d = 20$ cm are shown in Fig. 7. At a relatively far distance even still within the radiating near field, the peak incident power density can be well characterized by the far-field pattern [40], [41]. This means, particularly for small arrays, the maximum exposure that determines P_{MPT}, for $d = 20$ cm is approximately inversely proportional to the

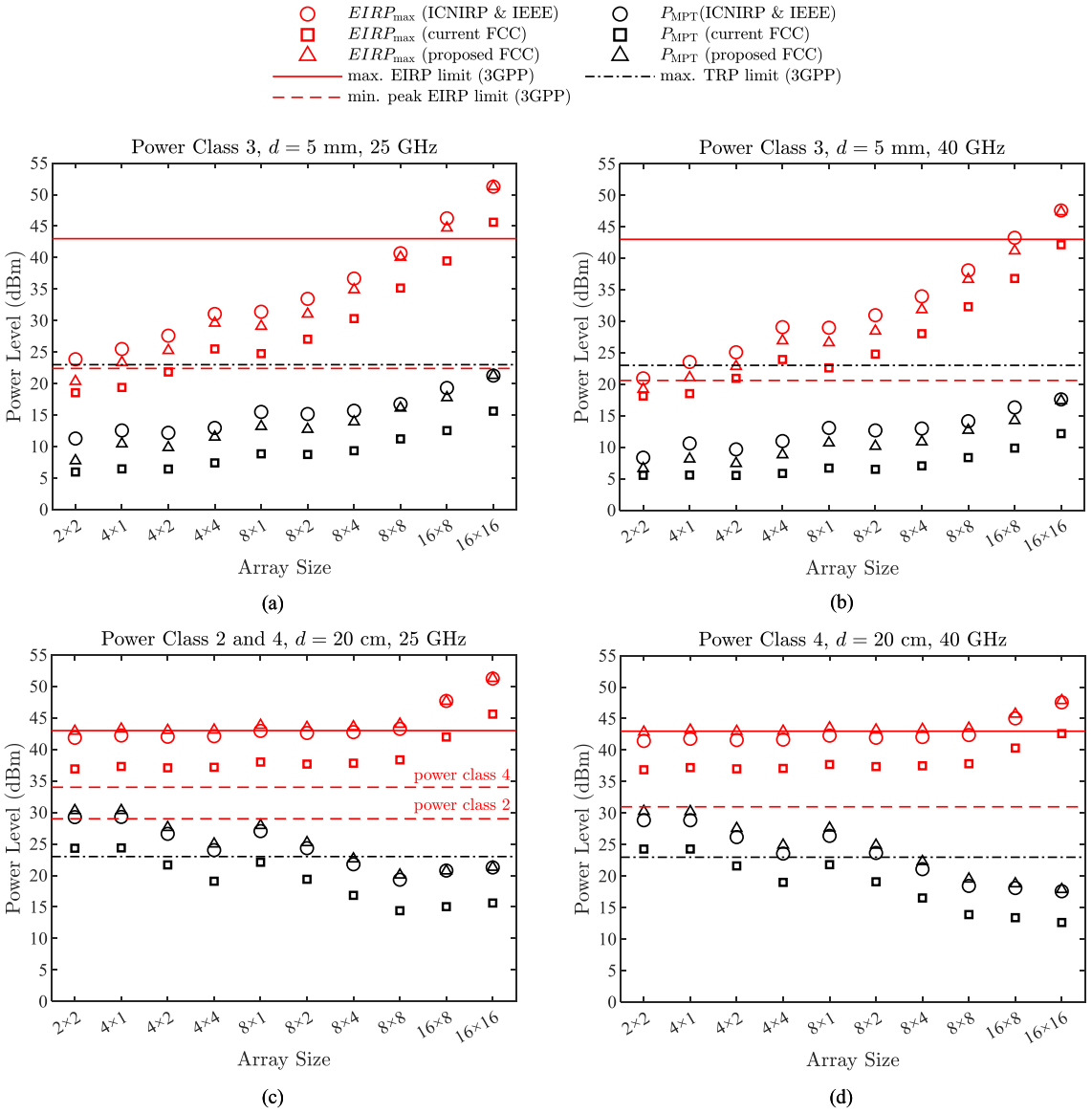

FIGURE 8. P_{MPT} and $EIRP_{max}$ levels to comply with the incident power density limits set by the ICNIRP, IEEE, current FCC, and proposed FCC for (a) UE power class 3 at 25 GHz, (b) UE power class 3 at 40 GHz, (c) UE power classes 2 and 4 at 25 GHz, and (d) UE power class 4 at 40 GHz. The red solid lines indicate the 3GPP maximum EIRP limits. The red dashed lines indicate the 3GPP minimum peak EIRP limits. The black dash-dotted lines indicate the 3GPP maximum TRP limits. The black and red makers represent the P_{MPT} and $EIRP_{max}$ levels according to the incident power density limits, respectively.

antenna gain, which is frequency-independent for the same array topology. Therefore, for small arrays, the P_{MPT} level is less relevant to the frequency. For large arrays such as the 16×8 and 16×16 arrays, the distance where the peak incident power density can be well approximated by the far-field pattern may be far beyond $d = 20$ cm as shown in Fig. 10 in Appendix A, and thus the results show a frequency-dependent behavior. In addition, the location of maximum exposure of large arrays, which determines P_{MPT}, is farther than 20 cm at low frequencies. This results in similar P_{MPT} levels between $d = 20$ cm and $d = 5$ mm for large arrays. The P_{MPT} levels for the ICNIRP and IEEE limits are identical, as suggested in the above section.

C. MAXIMUM EQUIVALENT ISOTROPICALLY RADIATED POWER

The P_{MPT} and $EIRP_{max}$ levels due to the RF EMF exposure restrictions are compared with the 3GPP UE power requirements in FR2, as shown in Fig. 8. The results of 25 GHz and 40 GHz are selected for the bands 24.25–29.5 GHz and 37–40 GHz, respectively. In comparison, the total efficiency of antenna arrays is assumed to equal to 1 when comparing P_{MPT} with the TRP limits.

For UE power class 3, at both 25 GHz and 40 GHz, the $EIRP_{max}$ levels of small arrays (2×2, 4×1, and 4×2) are close to the 3GPP minimum peak EIRP requirements. The $EIRP_{max}$ levels of very large arrays (16×8 and 16×16) may

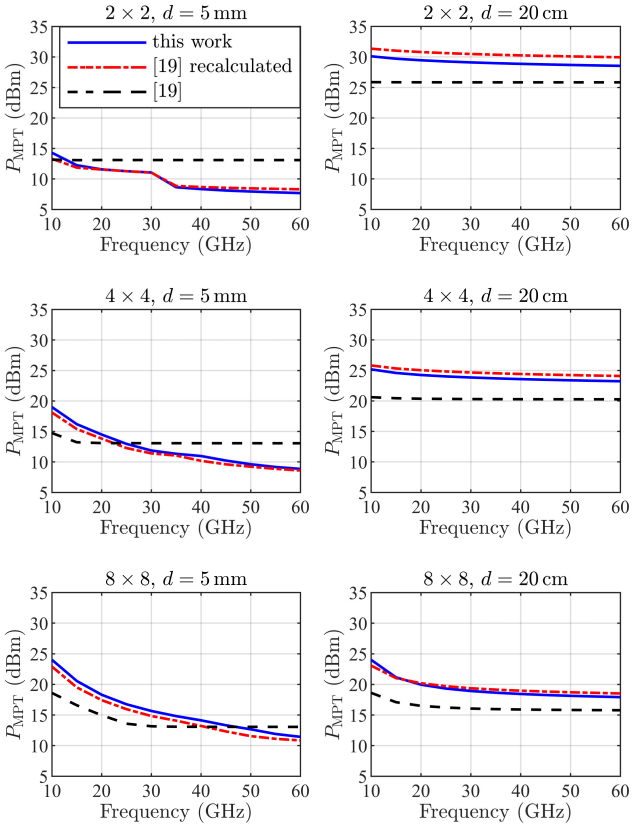

FIGURE 9. Comparison of P_{MPT} obtained in this paper for the updated ICNIRP incident power density limits (blue lines), the recalculated P_{MPT} using the dipole array model in [19] for the revised ICNIRP incident power density limits (red dash-dotted lines), and P_{MPT} extracted from [19] with the dipole array model for the incident power density limits in the ICNIRP 1998 guidelines [16] (black dashed lines). The P_{MPT} levels are compared for $d = 5$ mm and $d = 20$ cm, and for 2 × 2, 4 × 4, and 8 × 8 arrays.

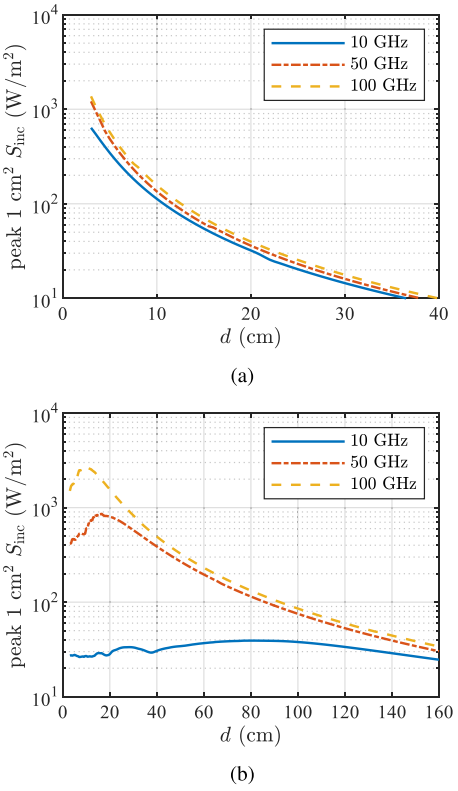

FIGURE 10. The peak 1 cm^2 spatial-average incident power density as distance varies, calculated with A-solver for (a) 2 × 2 and (b) 16 × 16 array at 10 GHz, 50 GHz, and 100 GHz.

surpass the 3GPP maximum EIRP limits if the antenna arrays transmit with P_{MPT}.

For power class 4 at both 25 GHz and 40 GHz, P_{MPT} of the array sizes smaller than 8 × 4 is likely to exceed the 3GPP maximum TRP limits. If scaling down the P_{MPT} levels of those arrays to meet the 3GPP TRP limits, the resultant $EIRP_{max}$ values will still locate within the required 3GPP peak EIRP range. This suggests that once the 3GPP requirements on maximum TRP, minimum peak EIRP, and maximum EIRP levels are fulfilled, the RF EMF exposure compliance may not be the limiting factor for the power levels of UE power classes 2 and 4 for $d = 20$ cm.

Using the P_{MPT} results in Fig. 6 and Fig. 7, the $EIRP_{max}$ results for the entire 10 GHz to 100 GHz range are provided in Fig. 13 and Fig. 14 in Appendix D. As 3GPP currently only specifies TRP and EIRP requirements in FR2 while it has not specified them yet in other parts of the spectrum above 6 GHz, the provided $EIRP_{max}$ levels are only used as indicators for coverage and link budget analysis. If new TRP and EIRP limits are specified or readers want to impose the FCC EIRP limits for other frequencies, a similar analysis can be performed using the data provided in Figs. 6, 7, 13, and 14.

IV. DISCUSSION

In Fig. 8(a) and (b), the $EIRP_{max}$ levels for the 2 × 2 and 4 × 1 arrays are a few dB below the 3GPP minimum EIRP limits. However, there are a few factors, which can affect the P_{MPT} and $EIRP_{max}$ levels for RF EMF compliance given the same antenna array model. As in [19], the RF EMF exposure assessment in this paper is made under the assumption of 100 % uplink duty cycle. If the UE employs time division duplex (TDD), the TDD downlink/uplink ratio must be considered when evaluating the time-averaged RF EMF exposure. For example, P_{MPT} and $EIRP_{max}$ in Fig. 8 should be scaled up by 3 dB if a 50 % uplink duty cycle is applied, and 6 dB if a 25 % uplink duty cycle is applied. The higher P_{MPT} and $EIRP_{max}$ levels can also be achieved if UE can dynamically control the time-averaged radiated power, but this needs further study also with respect to the energy density limits (averaging time < 6 minutes). It is pointed out in [21] that in a realistic product environment, a higher P_{MPT} and $EIRP_{max}$ can also be expected because a realistic antenna integration environment will guide and scatter the electromagnetic energy to unwanted directions (therefore lowering the spatial-average power density) and also cause a higher loss in materials. It also shows in [21] that a larger element spacing can reduce the maximum peak spatial-average incident power density at close distances, though grating lobes might appear. By taking the aforementioned factors into consideration, it is expected that both 2 × 2

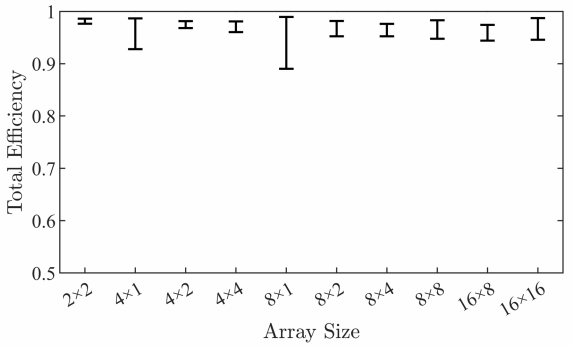

FIGURE 11. Ranges of the total efficiency of the antenna arrays as progressive phase difference β_x varies within $[0, \pi]$.

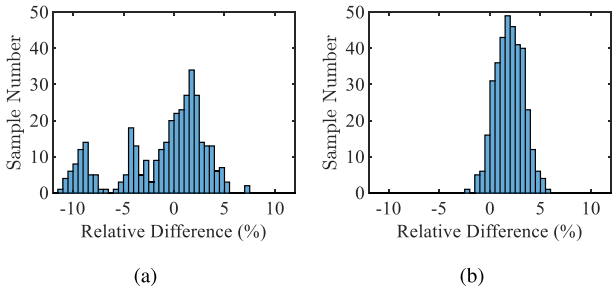

FIGURE 12. The distribution for the relative difference between the maximum peak spatial-average S_{inc} computed by the T-solver and that by the I-solver with the equivalent field sources within $\lambda_0/4 < d < \lambda_0$. The averaging area is (a) 1 cm^2 and (b) 4 cm^2. 360 samples in total are tested.

and 4×1 antenna arrays can meet EMF exposure requirements and 3GPP power/EIRP requirements simultaneously for UE power class 3.

A comparison between the P_{MPT} levels obtained in this paper and the P_{MPT} levels obtained using the antenna model in [19] is shown in Fig. 9. P_{MPT} for the reflector-based dipole array with $0.50\lambda_0$ element spacing was recalculated according to the revised ICNIRP power density limits for $d = 5$ mm and $d = 20$ cm, and for 2×2, 4×4, and 8×8 arrays. The comparison between the results of two works using different antenna elements, element spacing, and software tools suggest that the P_{MPT} levels are to a larger extent determined by the array topology, if other conditions are the same (see blue lines and red dash-dotted lines). In Fig. 9, the results computed in [19] for the incident power density limits according to the ICNIRP 1998 guidelines [16] (i.e., the incident power density averaged over 20 cm^2 should not exceed 10 W/m^2 for general public) are also presented for comparison (see black dashed lines). For $d = 5$ mm, slightly higher P_{MPT} levels towards the transition frequency, at which the relevant exposure quantity changes from the specific absorption rate (SAR) to power density, go in the right direction to resolve the discontinuity in P_{MPT} previously described in literature. Slightly lower P_{MPT} levels are observed at higher frequencies due to reduction in the averaging area. For $d = 20$ cm, as the fields around the peak are more or less uniform, the peak spatial-average incident power density is largely determined by the limit values ($55 f_{\mathrm{G}}^{-0.177}$ W/m^2 versus 10 W/m^2) rather than the size of averaging area. Thus, the revised ICNIRP limits imply slightly higher P_{MPT} levels for $d = 20$ cm.

When comparing array configurations with the same number of elements (e.g., 2×2 with 4×1), the one-dimensional arrays allow for a larger P_{MPT} of few dB as shown in Fig. 6.

The analysis in this paper has been conducted for UE operating within a single band at mmWave frequencies. If the UE is capable of transmitting with different bands simultaneously, for example above and below 6 GHz, the cumulative EMF exposure for all bands needs to be addressed by the compliance testing (see e.g., [42]).

V. CONCLUSION

The P_{MPT} and $EIRP_{\mathrm{max}}$ levels for different typical sizes of antenna arrays ranging from 2×2 to 16×16 have been assessed for 5G UE in the frequency range from 10 GHz to 100 GHz, according to the recently revised incident power density limits specified by the ICNIRP and the IEEE. A similar analysis has been conducted considering the current and proposed FCC limits. Compared to the previous works, the latest available information regarding the incident power density limits, the wider frequency range, and a variety of antenna array topologies have been considered in this work, and a fast simulation scheme has been developed. The obtained P_{MPT} and $EIRP_{\mathrm{max}}$ have also been compared with 3GPP TRP and EIRP requirements on UE within the NR FR2 bands. For 3GPP FR2 UE power class 3 (handheld UE), the results and discussion suggest that investigated array topologies can meet both RF EMF exposure compliance requirements and 3GPP TRP/EIRP requirements. For 3GPP FR2 UE power class 2 (vehicular UE) and power class 4 (high power non-handheld UE) with $d = 20$ cm, once the 3GPP maximum TRP and maximum EIRP requirements are met, the RF EMF exposure restrictions may not be a limiting factor for the power levels. The presented results provide valuable input about 5G NR to manufacturers, network operators, and standardization bodies.

APPENDIX A

Fig. 10 shows the peak 1 cm^2 spatial-average incident power density changing with distance, calculated by the A-solver for 2×2 and 16×16 arrays at 10 GHz, 50 GHz, and 100 GHz. The RF EMF exposure of the 2×2 array shows a frequency-independent behavior at 20 cm, while for the 16×16 array, the maximum exposure occurs at different distances and clearly, it shows a frequency-dependent behavior at 20 cm.

APPENDIX B

Although the dimension of the patch element is reused for all sizes of arrays, the impedance match conditions are different when putting in different array environments. Fig. 11 shows the range of total efficiency of different arrays as progressive phase difference β_x varies within $[0, \pi]$. The results can be used in an approximate way when P_{MPT} is needed to scale down to TRP.

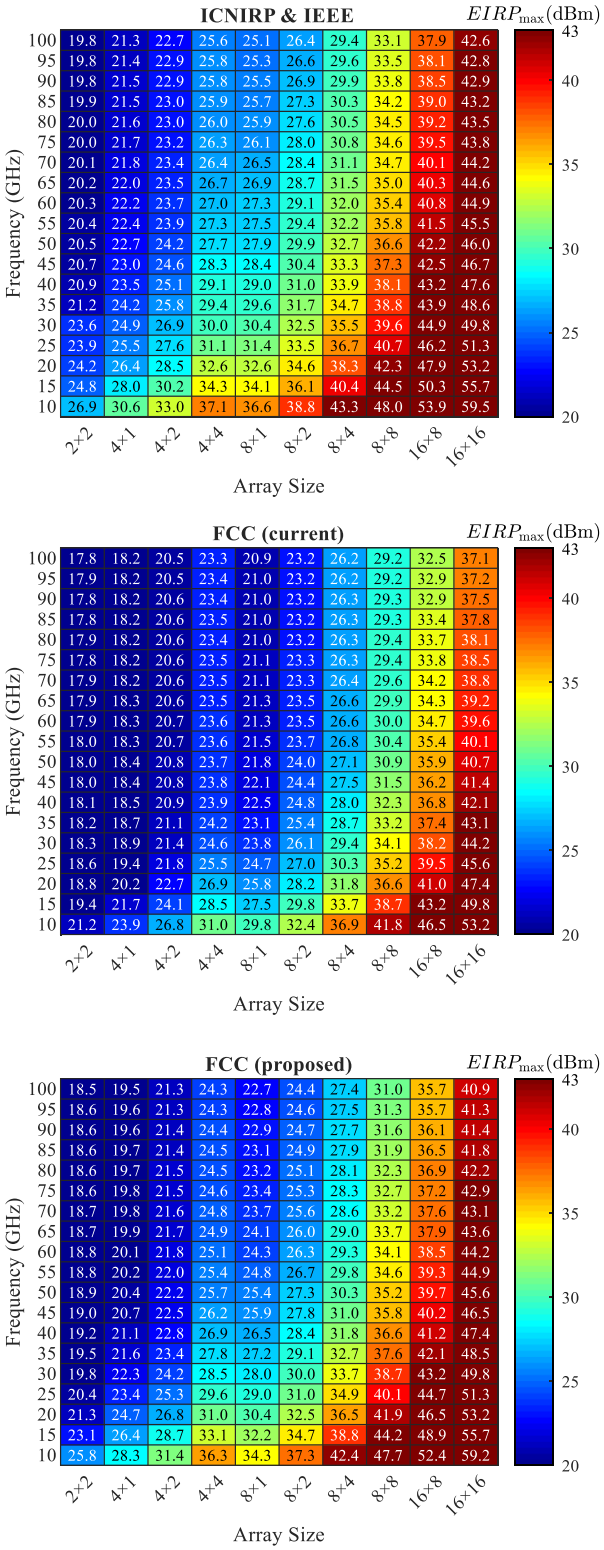

FIGURE 13. $EIRP_{max}$ levels for $d = 5$ mm to comply with the RF EMF exposure limits of ICNIRP, IEEE, FCC (current), and FCC (proposed).

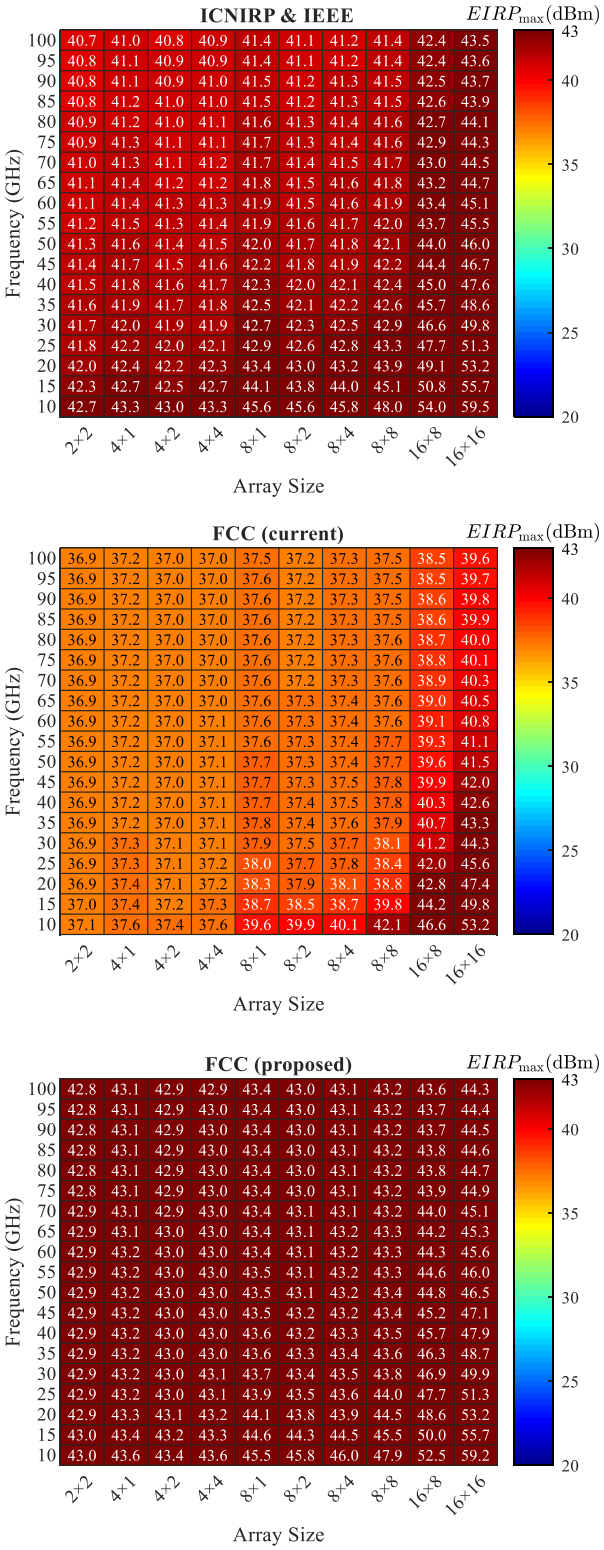

FIGURE 14. $EIRP_{max}$ levels for $d = 20$ cm to comply with the RF EMF exposure limits of ICNIRP, IEEE, FCC (current), and FCC (proposed).

APPENDIX C

Fig. 12 shows the distribution of the relative difference between S_{inc} calculated by the T-solver and that by the I-solver within $\lambda_0/4 < d < \lambda_0$. The maximum relative difference for the maximum peak S_{inc} averaged over 1 cm^2 and 4 cm^2 is 11.2 % and 5.6 %, respectively. The mean value of the relative difference for maximum peak S_{inc} averaged over 1 cm^2 and 4 cm^2 is 3.3 % and 2.0 %, respectively. Thus, the results from the I-solver using the equivalent field

sources can be considered comparable to the results directly computed from the T-solver.

APPENDIX D

Fig. 13 shows the $EIRP_{\max}$ levels for $d = 5$ mm to be compliant with the updated RF EMF exposure limits of ICNIRP, IEEE, FCC (current), and FCC (proposed), respectively. Fig. 14 shows the $EIRP_{\max}$ levels for $d = 20$ cm. These figures are useful for link budget and coverage analysis for 5G mmWave UE. Note the obtained $EIRP_{\max}$ is not considered with the 3GPP maximum EIRP restrictions.

ACKNOWLEDGMENT

(Wang He and Bo Xu contributed equally to this work.) The authors would like to thank the authors of [19] for providing their numerical models for comparison.

REFERENCES

[1] E. Dahlman, S. Parkvall, and J. Sköld, *5G NR: The Next Generation Wireless Access Technology*. New York, NY, USA: Academic, 2018.

[2] A. Osseiran, S. Parkvall, P. Persson, A. Zaidi, S. Magnusson, and K. Balachandran, "5G wireless access: An overview," Ericsson, Stockholm, Sweden, White Paper 1/28423-FGB1010937, Apr. 2020.

[3] T. S. Rappaport, S. Sun, R. Mayzus, H. Zhao, Y. Azar, K. Wang, G. N. Wong, J. K. Schulz, M. Samimi, and F. Gutierrez, "Millimeter wave mobile communications for 5G cellular: It will work!" *IEEE Access*, vol. 1, pp. 335–349, 2013.

[4] J. Helander, K. Zhao, Z. Ying, and D. Sjoberg, "Performance analysis of millimeter-wave phased array antennas in cellular handsets," *IEEE Antennas Wireless Propag. Lett.*, vol. 15, pp. 504–507, 2016.

[5] S. Zhang, X. Chen, I. Syrytsin, and G. F. Pedersen, "A planar switchable 3-D-coverage phased array antenna and its user effects for 28-GHz mobile terminal applications," *IEEE Trans. Antennas Propag.*, vol. 65, no. 12, pp. 6413–6421, Dec. 2017.

[6] K. Zhao, S. Zhang, Z. Ho, O. Zander, T. Bolin, Z. Ying, and G. F. Pedersen, "Spherical coverage characterization of 5G millimeter wave user equipment with 3GPP specifications," *IEEE Access*, vol. 7, pp. 4442–4452, 2019.

[7] I. Syrytsin, S. Zhang, G. F. Pedersen, and A. S. Morris, "Compact quad-mode planar phased array with wideband for 5G mobile terminals," *IEEE Trans. Antennas Propag.*, vol. 66, no. 9, pp. 4648–4657, Sep. 2018.

[8] W. Hong, K.-H. Baek, Y. Lee, Y. Kim, and S.-T. Ko, "Study and prototyping of practically large-scale mmWave antenna systems for 5G cellular devices," *IEEE Commun. Mag.*, vol. 52, no. 9, pp. 63–69, Sep. 2014.

[9] M. Stanley, Y. Huang, H. Wang, H. Zhou, A. Alieldin, and S. Joseph, "A capacitive coupled patch antenna array with high gain and wide coverage for 5G smartphone applications," *IEEE Access*, vol. 6, pp. 41942–41954, 2018.

[10] N. Ojaroudiparchin, M. Shen, S. Zhang, and G. F. Pedersen, "A switchable 3-D-coverage-phased array antenna package for 5G mobile terminals," *IEEE Antennas Wireless Propag. Lett.*, vol. 15, pp. 1747–1750, 2016.

[11] Y. Luo, J. Xu, Y. Chen, Y. Sun, B. Xu, S. Xu, and G. Yang, "A zero-mode induced mmWave patch antenna with low-profile, wide-bandwidth and large-angle scanning for 5G mobile terminals," *IEEE Access*, vol. 7, pp. 177607–177615, 2019.

[12] *IEEE Standard for Safety Levels With Respect to Human Exposure to Electric, Magnetic, and Electromagnetic Fields, 0 Hz to 300 GHz*, IEEE Standard C95.1-2019, Feb. 2019.

[13] *IEEE Standard for Safety Levels With Respect to Human Exposure to Human Exposure to Radio Frequency Electromagnetic Fields, 3 kHz to 300 GHz*, IEEE Standard C95.1-2005, Oct. 2005.

[14] *IEEE Standard for Safety Levels With Respect to Human Exposure to Human Exposure to Electromagnetic Fields, 0–3 kHz*, IEEE Standard C95.6-2002, Sep. 2002.

[15] International Commission on Non-Ionizing Radiation Protection (ICNIRP), "Guidelines for limiting exposure to electromagnetic fields (100 kHz to 300 GHz)," *Health Phys.*, vol. 118, no. 5, pp. 483–524, May 2020.

[16] The International Commission on Non-Ionizing Radiation Protection, "Guidelines for limiting exposure to time-varying electric, magnetic, and electromagnetic fields (up to 300 GHz)," *Health Phys.*, vol. 74, no. 4, pp. 494–522, Apr. 1998.

[17] International Commission on Non-Ionizing Radiation Protection, "Guidelines for limiting exposure to time-varying electric and magnetic fields (1 Hz to 100 kHz)," *Health Phys.*, vol. 99, no. 6, pp. 818–836, 2010.

[18] *User Equipment (UE) Radio Transmission and Reception; Part 2: Range 2 Standalone*, document 3GPP TS 38.101-2 v15.9.1, Apr. 2020.

[19] B. Thors, D. Colombi, Z. Ying, T. Bolin, and C. Tornevik, "Exposure to RF EMF from array antennas in 5G mobile communication equipment," *IEEE Access*, vol. 4, pp. 7469–7478, 2016.

[20] K. Zhao, Z. Ying, and S. He, "EMF exposure study concerning mmWave phased array in mobile devices for 5G communication," *IEEE Antennas Wireless Propag. Lett.*, vol. 15, pp. 1132–1135, 2016.

[21] B. Xu, K. Zhao, Z. Ying, D. Sjoberg, W. He, and S. He, "Analysis of impacts of expected RF EMF exposure restrictions on peak EIRP of 5G user equipment at 28 GHz and 39 GHz bands," *IEEE Access*, vol. 7, pp. 20996–21005, 2019.

[22] W. He, B. Xu, M. Gustafsson, Z. Ying, and S. He, "RF compliance study of temperature elevation in human head model around 28 GHz for 5G user equipment application: Simulation analysis," *IEEE Access*, vol. 6, pp. 830–838, 2018.

[23] Y. Hashimoto, A. Hirata, R. Morimoto, S. Aonuma, I. Laakso, K. Jokela, and K. R. Foster, "On the averaging area for incident power density for human exposure limits at frequencies over 6 GHz," *Phys. Med. Biol.*, vol. 62, no. 8, pp. 3124–3138, Apr. 2017.

[24] B. Xu, K. Zhao, B. Thors, D. Colombi, O. Lundberg, Z. Ying, and S. He, "Power density measurements at 15 GHz for RF EMF compliance assessments of 5G user equipment," *IEEE Trans. Antennas Propag.*, vol. 65, no. 12, pp. 6584–6595, Dec. 2017.

[25] B. Xu, M. Gustafsson, S. Shi, K. Zhao, Z. Ying, and S. He, "Radio frequency exposure compliance of multiple antennas for cellular equipment based on semidefinite relaxation," *IEEE Trans. Electromagn. Compat.*, vol. 61, no. 2, pp. 327–336, Apr. 2019.

[26] K. Sasaki, K. Li, J. Chakarothai, T. Iyama, T. Onishi, and S. Watanabe, "Error analysis of a near-field reconstruction technique based on plane wave spectrum expansion for power density assessment above 6 GHz," *IEEE Access*, vol. 7, pp. 11591–11598, Feb. 2019.

[27] S. Pfeifer, E. Carrasco, P. Crespo-Valero, E. Neufeld, S. Kuhn, T. Samaras, A. Christ, M. H. Capstick, and N. Kuster, "Total field reconstruction in the near field using pseudo-vector E-field measurements," *IEEE Trans. Electromagn. Compat.*, vol. 61, no. 2, pp. 476–486, Apr. 2019.

[28] J. Lundgren, J. Helander, M. Gustafsson, D. Sjöberg, B. Xu, and D. Colombi, "Near-field measurement and calibration technique for RF EMF exposure assessment of mm-wave 5G devices," *IEEE Antennas Propag. Mag.*, early access, doi: 10.1109/MAP.2020.2988517.

[29] M. Nesterova, S. Nicol, and Y. Nesterova, "Evaluating power density for 5G applications," in *Proc. IEEE 5G World Forum (5GWF)*, Jul. 2018, pp. 347–350.

[30] *FCC, Code of Federal Regulation Title 47, Section 1.1310, Radio Frequency Radiation Exposure Limits*, FCC, Washington, DC, USA, 1996.

[31] FCC. (Oct. 2018). *RF Exposure Procedures*. [Online]. Available: https://transition.fcc.gov/oet/ea/presentations/files/oct18/5.2-RF_Exposure_Procedures-JN.PDF

[32] FCC. (Apr. 2019). *RF Exposure Procedures*. [Online]. Available: https://transition.fcc.gov/oet/ea/presentations/files/apr19/4.0-RF-Exposure-Panel-FINAL.pdf

[33] *Resolution of Notice of Inquiry, Second Report and Order, Notice of Proposed Rulemaking, and Memorandum Opinion and Order*, document FCC 19-126, Dec. 2019.

[34] TCB workshop, FCC. (Nov. 2017). *RF Exposure Procedures*. [Online]. Available: https://transition.fcc.gov/oet/ea/presentations/files/nov17/71-RF-Exposure-TCB-Slides-OctNov-2017-KC.pdf

[35] *FCC, Code of Federal Regulation, Title 47, Section 2.1093, Radiofrequency Radiation Exposure Evaluation: Portable Devices*, FCC, Washington, DC, USA, 2019.

[36] *FCC, Code of Federal Regulation, Title 47, Section 2.1091, Radiofrequency Radiation Exposure Evaluation: Mobile Devices*, FCC, Washington, DC, USA, 2019.

[37] D. Colombi, B. Thors, C. Tornevik, and Q. Balzano, "RF energy absorption by biological tissues in close proximity to millimeter-wave 5G wireless equipment," *IEEE Access*, vol. 6, pp. 4974–4981, 2018.
[38] *CST Studio Suite*. Accessed: Mar. 10, 2020. [Online]. Available: https://www.3ds.com/products-services/simulia/products/cst-studio-suite/
[39] *MATLAB*. Accessed: Mar. 10, 2020. [Online]. Available: https://www.mathworks.com/products/matlab.html
[40] B. Xu, D. Colombi, and C. Tornevik, "EMF exposure assessment of massive MIMO radio base stations based on traffic beam pattern envelopes," in *Proc. 14th Eur. Conf. Antennas Propag. (EuCAP)*, Mar. 2020, pp. 1–5.
[41] B. Derat, "5G antenna characterization in the far-field: How close can far-field be?" in *Proc. IEEE Int. Symp. Electromagn. Compat. IEEE Asia–Pacific Symp. Electromagn. Compat. (EMC/APEMC)*, Singapore, May 2018, pp. 959–962.
[42] *Guidance for Evaluating Exposure From Multiple Electromagnetic Sources*, document IEC 62 630, Oct. 2010.

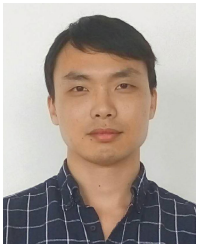

WANG HE received the B.E. degree in information engineering and the Ph.D. degree in optical engineering from Zhejiang University, Hangzhou, Zhejiang, China, in 2015 and 2020, respectively. His current research interests include electromagnetics and antenna design.

BO XU (Member, IEEE) received the B.E. degree in information engineering and the Ph.D. degree in optical engineering from Zhejiang University, Hangzhou, Zhejiang, China, in 2010 and 2017, respectively. He is currently pursuing the Joint Ph.D. Program with the Department of Electromagnetic Engineering, KTH Royal Institute of Technology, Stockholm, Sweden, and the Centre for Optical and Electromagnetic Research, Zhejiang University. He was a Visiting Student with the Department of Electrical and Information Technology, Lund University, Lund, Sweden, in 2016 and 2017.

Since 2018, he has been an Experienced Researcher with Ericsson Research, Ericsson AB, Stockholm, Sweden. His research interests include electromagnetic field health and safety, antenna design, and measurements.

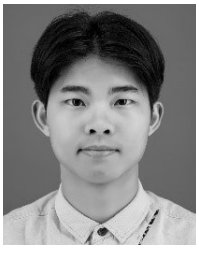

YUANQING YAO received the B.E. degree in electronic information science and technology from the Hefei University of Technology, Hefei, China, in 2018. He is currently pursuing the Ph.D. degree with the Centre for Optical and Electromagnetic Research, Zhejiang University, Hangzhou, China. His current research interests include antenna design and radio frequency electromagnetic field exposure.

DAVIDE COLOMBI received the M.Sc. degree (summa cum laude) in telecommunication engineering from the Politecnico di Milano, Italy, in 2009. Since 2009, he has been with Ericsson Research, Stockholm, Sweden, where he is currently working with research related to radio frequency exposure from wireless communication equipment, particularly for 5G. He has contributed to the development of IEC, ITU, and the IEEE standards on the assessment of radio frequency exposure from wireless equipment as an expert, an editor, and a convener. He was a recipient of the 2018 IEC 1906 Award.

ZHINONG YING (Senior Member, IEEE) joined Ericsson AB, Lund, Sweden, in 1995. He was a Senior Specialist, in 1997, and an Expert, in 2003, in his engineer career. He has been an Antenna Expert with Ericsson, Sony Ericsson, and Sony. Since 2001, he has been a Guest Professor with the Joint Research Centre, KTH Royal Institute of Technology, Stockholm, Sweden, and Zhejiang University, Hangzhou, China. He is currently a Principle Engineer of antenna technology with the Connectivity Technology Laboratory, Sony Research Center in Sweden. He is also a Distinguished Researcher with the whole Sony Group. He has authored or coauthored over 160 articles in various kinds of journal, conference, and industry publications. He holds more than 160 patents and pending in the antennas and new generation wireless network areas. He contributed several book chapters on mobile antenna, small antenna, and multiple-input and multiple-output (MIMO) antennas in *Mobile Antenna Handbook 3rd edition* edited H. Fujimoto and *Handbook of Antenna Technologies* edited by Z. N. Chen. He had contributed a lot of work in antenna designs and evaluation methods for the mobile industry. He has also involved in the evaluation of bluetooth technology, which was invented by Ericsson. His current research interests include small antennas, broad and multiband antenna, multichannel antenna (MIMO) systems, antenna for body area networks, antenna and propagation in fifth-generation mobile networks, including massive MIMO and mm-wave, near-field exposure and human body effects, and measurement techniques. From 2004 to 2007, he was a member of the Scientific Board of Antenna Center of Excellent in the European 6th Frame Program. He was a recipient of the Best Invention Award at Ericsson Mobile, in 1996, the Key Performer Award at Sony Ericsson, in 2002, the President Award at Sony Ericsson, in 2004, for his innovative contributions, the Distinguish Engineer title at Sony Group, in 2013. He served as a TPC Co-Chairman for the International Symposium on Antenna Technology, in 2007. He served as an Associate Editor of *AWPL*. He served as a Reviewer for several academic journals.

SAILING HE (Fellow, IEEE) received the Licentiate of Technology and Ph.D. degrees in electromagnetic theory from the Royal Institute of Technology (KTH), Stockholm, Sweden, in 1991 and 1992, respectively. Since 1992, he has been working with the Royal Institute of Technology, as an Assistant Professor, an Associate Professor, and a Full Professor. He is currently a Distinguished Professor with Zhejiang University. He is also the Director of the Joint Research Center (JORCEP) with KTH and ZJU. He has first-authored one monograph and authored/coauthored about 600 articles in refereed international journals. His current research interests include applied electromagnetics, optoelectronics, and sensing applications. He is a Fellow of the Optical Society of America (OSA), the International Society for Optical Engineering (SPIE), and the Electromagnetics Academy.